$CHPh$[14b] and $(CH_2Ph)Cl(\eta^5\text{-}C_5Me_5)Ta{=}CHPh$.[23a] Our results imply that the metal-carbene bonds of these two compounds are weaker than their alkylidene counterparts. An X-ray crystal structure on $(CH_2Ph)Cp_2Ta{=}CHPh$ supports this idea; the Ta=C bond distance of 2.07 Å is 0.17 Å shorter that a Ta-C single bond, but 0.05 Å longer than a typical Ta=C double bond. A weaker than normal Ta=C bond would make these two compounds interesting candidates for catalytic studies.

Conclusion

Through the use of a properly designed basis set (doubleζ in the metal carbene, minimal basis elsewhere) and limited electron correlation (GMO and CI methods) within the double bond, reasonable electron densities and dissociation energies can be calculated on large metal-carbene systems.

A calculation on ethylene using the same techniques and basis set yields a bond dissociation energy only 4 kcal mol^{-1} less than the experimental estimate of 163 kcal mol^{-1}. A partial geometry optimization on $CpCl_2Nb{=}CH_2$ indicates this electron-deficient complex has a Nb=C bond distance, 1.99 Å, similar to well-characterized 18-electron complexes. The calculated rotational barrier of the methylene in $CpCl_2Nb{=}CH_2$ is 14.6 kcal mol^{-1}, in good agreement with experimental determinations of similar compounds. This value also sets a lower limit on the π bond energy of $CpCl_2Nb{=}CH_2$, since the π bond is only partially broken when the methylene group is rotated 90°. The other three metal carbenes studied have bond dissociation energies 14 to 18 kcal mol^{-1} less than $CpCl_2Nb{=}CH_2$, apparently because of weaker π bonds in these complexes.

Several independent techniques (dissociation energies, single electron valence bond density plots, atomic deformation densities, fragment deformation densities, molecular orbital diagrams, and fragment analysis of molecular orbitals) illustrate the electronic difference between Fischer-type metal carbenes and Schrock-type tantalum carbenes. The former bind datively as singlet fragments, whereas the latter bind covalently as triplet fragments.

Acknowledgment. This work was supported by the National Science Foundation (CHE79-20993 and CHE83-09936) and the National Resource for Computation in Chemistry (National Science Foundation Grant No. CHE77-21305). The authors thank Professor R. Schrock for the opportunity to present this work in the Symposium on the Chemistry of Unsaturated Metal-Carbon Bonds at the 184th American Chemical Society Meeting, Kansas City, Sept. 12-17, 1982.

Registry No. 3, 88589-51-9; **4**, 88609-69-2; **5**, 88589-52-0; **6**, 88589-53-1; **7**, 74-85-1.

(34) (a) Friedrich, P.; Besl, G.; Fischer, E. O.; Huttner, G. *J. Organomet. Chem.* **1977**, *139*, C68. (b) Redhouse, A. D. *Ibid.* **1975**, *99*, C29. Similar Fe compounds are also known; see Brookhart, M.; Tucker, J. R.; Husk, G. R. *J. Am. Chem. Soc.* **1981**, *103*, 979. Brookhart, M.; Tucker, J. R.; Flood, T. C.; Jensen, J. *Ibid.* **1980**, *102*, 7802.

(35) Wolczanski, P. T.; Threlkel, R. S.; Bercaw, J. E. *J. Am. Chem. Soc.* **1979**, *101*, 218.

Calculation of Electron Tunneling Matrix Elements in Rigid Systems: Mixed-Valence Dithiaspirocyclobutane Molecules

David N. Beratan* and J. J. Hopfield†

Contribution No. 6850 from the Division of Chemistry and Chemical Engineering, California Institute of Technology, Pasadena, California 91125. *Received August 4, 1983*

Abstract: A semiempirical model is presented which predicts photoassisted electron-transfer rate dependence on distance for redox groups connected by rigid polymeric linkers. The model approximately reproduces the observed decay of the optical tunneling matrix element with distance found for the rigid ruthenium dithiaspiro mixed-valence complexes of Stein, Lewis, Seitz, and Taube.[1-3] The method calculates the through-bond propagation of the wave function tail, by a method which emphasizes obtaining the correct distance dependence of the tunneling matrix element for these weakly interacting donor-acceptor complexes. The method also allows prediction of the magnitude of the matrix element, the importance of hole or electron tunneling in the transport process, the effect of donor and acceptor redox potential on the matrix element, and the thermal tunneling matrix element for these and other compounds.

Introduction

Electron-transfer theory predicts an approximately exponential decrease in electron-transfer rate with distance when the donor and acceptor weakly interact.[4-6] Only recently, however, have rigid molecules with weakly interacting electron donor and acceptor groups become available.[1-3,7,8] Predictions of transfer rates, qualitative in the past, must be refined to treat this new class of compounds. A series of mixed-valence ruthenium molecules (I, II, III) was recently synthesized and studied by Stein, Lewis, Seitz, and Taube.[2,3]

Interaction between the metal ions is believed to be rather weak and to involve through-bond rather than through-space interactions.[2,3,9] If the interaction between donor and acceptor is indeed weak, one may imagine that relaxation of vibrational modes in the molecule and of the solvent around the odd electron (vibronic coupling) stabilizes the localization. This relaxation provides a deeper well for the electron on one side of the molecule compared to the otherwise equivalent site. Hence one finds, for a short time at least, a ground state for the odd electron localized on one relaxed

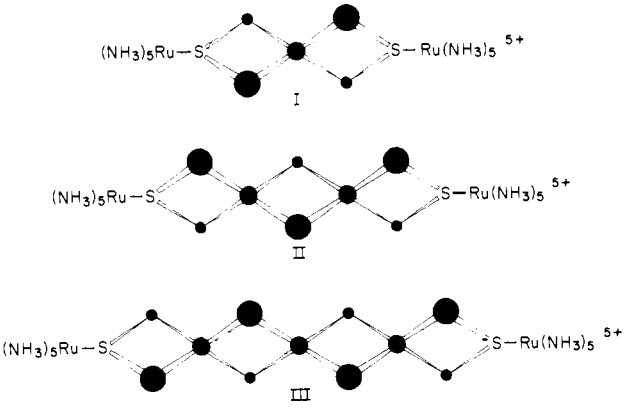

† Also California Institute of Technology, Division of Biology, and Bell Laboratories, Murray Hill, NJ 07974.

(1) Taube, H. In "Tunneling in Biological Systems"; Chance, B., DeVault, D. C., Frauenfelder, H., Marcus, R. A., Schreiffer, J. R., Sutin, N., Eds.; Academic Press: New York, 1979, pp 173-199.

(2) Stein, C. A.; Taube, H. *J. Am. Chem. Soc.* **1981**, *103*, 693-695.

(3) Stein, C. A.; Lewis, N. A.; Seitz, G. *J. Am. Chem. Soc.* **1982**, *104*, 2596-2599.

0002-7863/84/1506-1584$01.50/0

metal–ligand group. An unoccupied excited state for an electron localized on the unrelaxed site also exists.[10] Therefore, a charge-transfer optical absorption between these states can be found. For I, II, and III a charge-transfer band was found (ϵ = 43, 9, 2.3 M^{-1} cm^{-1}, respectively). The extinction coefficient of this band is related to the tunneling matrix element in the Gaussian approximation when the donor and acceptor are identical as shown in eq 1.[10]

$$\epsilon(E_0) = \zeta(|T_{ab}|^2/E_0)(a^2/\sigma)G \quad (1)$$

$$\zeta = [2n/(n^2 + 1)](2\pi^2/3)(N_0/2300)(e^2/\hbar c)(1/2\pi)^{1/2} = 4.60 \times 10^{18}\ M^{-1}\ cm^{-3} \text{ when } n = 1.53$$

$$G = \exp[-(E_0 - \Delta)^2/2\sigma^2]$$

E_0 is the energy of the photon, e is the charge on the electron, a is the donor acceptor distance, T_{ab} is the optical tunneling matrix element, n is the index of refraction of the sample, N_0 is Avogadro's number, $\hbar$ is Planck's constant/2π, c is the speed of light, Δ is the reorganizational energy, and σ is the half-width of the charge-transfer band at 0.61 maximum. A first-order perturbation treatment of weakly interacting donor and acceptor groups predicts the electric dipole matrix element of the charge-transfer band is given by[10]

$$\langle\psi_g|e\vec{x}|\psi_{ex}\rangle = eaT_{ab}/(E_g - E_{ex}) \quad (2)$$

ψ_g and ψ_{ex} are the ground- and excited-state wave functions, respectively. $\vec{x}$ is the position operator. Equation 1 allows the calculation of $|T_{ab}|$, the optical tunneling matrix element, from the experimentally determined extinction coefficient. $|T_{ab}|$ contains the distance dependence of the electron-transfer rate. Fermi's "golden rule" predicts that the transfer rate depends on the square of $|T_{ab}|$.[11] We develop a method of finding the appropriate ground- and excited-state wave functions which allows the independent prediction of T_{ab}. The most important capability of this method is its ability to predict the distance dependence of T_{ab} for donors and acceptors of given redox energy. The relevance of this method to electron transfer in proteins is also considered.

Theoretical Section

The problem of electron exchange between traps at fixed distance has been discussed recently by several authors.[12-17] Understanding how electron-transfer rates depend on molecular structure is essential for an understanding of biological electron-transfer reactions. This interest in the structure–function relationship forces us to first understand electron-transfer processes in "model compounds". T_{ab} depends critically on the overlap of the two localized wave functions and is difficult to calculate. These matrix elements depend on the details of what is usually an uninteresting chemical aspect of the electronic wave function, its tail. The wave-function tail decay can be significantly altered by changing the atoms between donor and acceptor. The problem of calculating tunneling matrix elements is, as yet, intractable using traditional ab initio methods for molecular structure determination. The choice of orbital basis set may severely alter the size of T_{ab}. Traditional variational methods, which optimize the energy of a state, are rather insensitive to the form of the small amplitude wave function tail. Variational methods can tolerate errors in the long-range behavior of the function because changes of these tails cause little change in the total energy of the state. We have chosen a semiempirical approach which assures the proper behavior of the wave function in the region between the electron traps where the wave function decay is rapid.

Periodic Approximation. The fundamental assumption which we make is that within the central region of the hydrocarbon linker the potential is periodic; i.e., at corresponding points of different rings the potential is equal. This assumption neglects the perturbing effects of the Coulombic potentials centered on the ruthenium atoms. As the experiments were performed in aqueous DCl, the dielectric screening is expected to shield the central atoms (at least 2.5 Å away) from this potential. The terminal sulfur orbitals perturb the potentials of the neighboring carbon atoms, causing them to differ somewhat from other secondary carbons in the center of the spiro ligand. This effect is expected to be small. Within the standard extended-Hückel theory, our periodic approximation is equivalent to choosing the same orbital exponents for each orbital of the same type.

Let us investigate the form of the wave function for a long chain of spiroalkane rings. Because the potential is periodic along this chain, the translation operator T commutes with the Hamiltonian $\mathcal{H}$ of the system in this region:

$$[\mathcal{H},T] = 0 \quad (3)$$

The wave function can then be chosen to be an eigenfunction of the translation operator, so:

$$T\psi = (\epsilon)\psi \quad (4)$$

$$T^2\psi = (\epsilon)^2\psi, \ldots$$

where ϵ is some number. We may solve the Schrödinger equation to find a relationship between ϵ and the energy of the states.[18] Truncating one end of the chain and adding special end orbitals does not change the energy–ϵ relationship since the *potential* in the central region is not changed by the truncation. Moreover, one can instead truncate the opposite end, add a different group here, and solve a different single "impurity" problem. Finally, one may truncate these single impurity wave functions and form a linear combination of these two single impurity chains. One is assured (within the LCAO approximation) of having a wave function with the correct behavior in the central region. The energy–ϵ relation true for the infinite spiro chain is also true for the finite molecule. This approach is equivalent to writing the Bloch states for a crystal in terms of some wave vector. Only after the boundary conditions of the crystal are considered, be they cyclic or not, do we obtain explicit values for the wave vector.

The problem of interactions between "special" groups embedded in otherwise normal solvent or crystal pervades chemistry. For example, theories of electronic excitation transfer parallel very closely the central ideas of electron transfer theory.[4,19,20] Koster and Slater studied the energetics of impurity levels in solids long ago.[21,22] Semiconductors doped with impurities are known to trap excitons (electron hole pairs) on these impurities or on neighboring impurities. Faulkner and Hopfield developed a theory of the optical properties for a class of these doped semiconductors.[23,24] These problems are cousins of the photoassisted electron-transfer problem.[10,25-27] A treatment of wave function propagation similar

(4) Hopfield, J. J. *Proc. Natl. Acad. Sci. U.S.A.* **1974**, *71*, 3640–3644.
(5) Jortner, J. *J. Chem. Phys.* **1976**, *64*, 4860–4867.
(6) Eyring, H.; Walter, J.; Kimball, G. E. "Quantum Chemistry"; Wiley: New York, 1944; Chapter XI.
(7) Calcaterra, L. T.; Closs, G. L.; Miller, J. R. *J. Am. Chem. Soc.* **1983**, *105*, 670–671.
(8) Pasman, P.; Koper, N. W.; Verhoeven, J. W. *Rech. Trav. Chim. Pays-Bas* **1982**, *101*, 363–364.
(9) Stein, C. A.; Lewis, N. A.; Seitz, G.; Baker, A. D. *Inorg. Chem.* **1983**, *22*, 1124–1228.
(10) Hopfield, J. J. *Biophys. J.* **1977**, *18*, 311–321.
(11) Mertzbacher, E. "Quantum Mechanics", 2nd ed., Wiley: New York, 1970.
(12) DeVault, D. *Q. Rev. Biophys.* **1980**, *13*, 387–564.
(13) Jortner, J. *Biochim. Biophys. Acta* **1980**, *594*, 193–230.
(14) Day, P. *Int. Rev. Phys. Chem.* **1981**, *1*, 149–193.
(15) Chance, B., DeVault, D. C., Frauenfelder, H., Marcus, R. A., Schrieffer, J. R., Sutin, N., Eds. "Tunneling in Biological Systems"; Academic Press: New York, 1979.
(16) Lippard, S. J., Ed. "Progress in Inorganic Chemistry"; Wiley: New York, 1983; Vol. 30.
(17) Larsson, S. *J. Am. Chem. Soc.* **1981**, *103*, 4034–4040.
(18) In the limit of a long chain or orbitals, we discover Bloch's theorem and allowed "bands" of energy eigenvalues for the very large number of eigenstates. See ref 33.
(19) Robinson, G. W.; Frosch, R. P. *J. Chem. Phys.* **1962**, *37*, 1962–1973.
(20) Robinson, G. W.; Frosch, R. P. *J. Chem. Phys.* **1963**, *38*, 1187–1203.
(21) Koster, G. F.; Slater, J. C. *Phys. Rev.* **1954**, *95*, 1167–1176.
(22) Koster, G. F.; Slater, J. C. *Phys. Rev.* **1954**, *96*, 1208–1223.
(23) Faulkner, R. A. *Phys. Rev.* **1968**, *175*, 991–1009.
(24) Faulkner, R. A.; Hopfield, J. J. In "Localized Excitations in Solids"; Wallis, R. F., Ed.; Plenum Press: New York, 1968; pp 218–238.
(25) Redi, M.; Hopfield, J. J. *J. Chem. Phys.* **1980**, *72*, 6651–6660.
(26) Hush, N. S. *Electrochim. Acta* **1968**, *13*, 1005–1023.

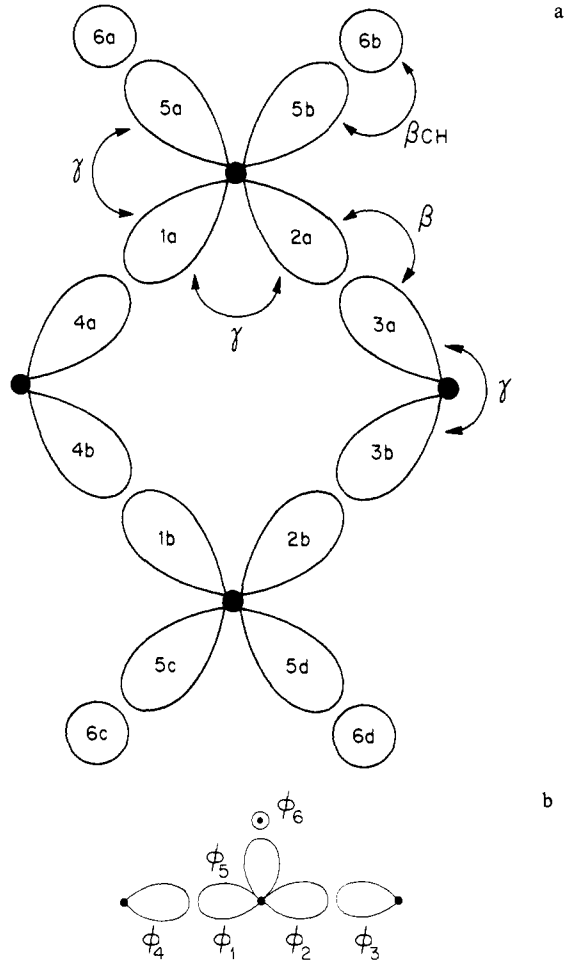

Figure 1. (a) The 16 orbitals of the unit cell are shown. Orbitals with equal integers are combined to form symmetrized orbitals. The orbital interactions are also shown. (b) The six symmetrized basis orbitals that comprise the unit cell are shown.

to ours was used by McConnell to model intramolecular thermally activated charge transfer between aromatic free radicals separated by flexible methylene bridges.[28] Morton-Blake recently used a related perturbational method to study defect states in polymers.[29] Koiller, Brandi, and Ferreira have studied simple impurity problems using a Green's function formulation.[30,31] Larsson has compared the distance dependnece of σ- and π-mediated transfer rates between metals.[32] Most of these methods are adaptations of the tight-binding method of calculating the band structure for crystalline solids.[33] They differ in their description of the "periodic" part and the boundary conditions of the problem.

Because we have already made severe restrictions on the form of the wave-function decay, we choose the most simple model of the Hamiltonian in the central region and of the unit cell. We select the one-electron Hamiltonian

$$\mathcal{H} = \sum_i \alpha_i a_i^+ a_i + \sum_{j>i}\sum_i \beta_{ij}(a_i^+ a_j + a_j^+ a_i) + \sum_{k>m}\sum_m \gamma_{km}(a_k^+ a_m + a_m^+ a_k) \quad (5)$$

where a^+ and a are the electron creation and annihilation operators, respectively.[34] i sums over all basis functions in the wave function. i and j are nearest-neighbor orbitals on adjacent nuclei. k and m are orbitals on the same nucleus. There are 12 sp^3 carbon orbitals and 4 hydrogen orbitals per spiroalkane unit cell. Assuming that the Ru atoms lie on the line of the sulfur atoms and quaternary carbons, the molecule has two mirror planes containing the metal atoms.[9] This assumption is reasonable if there is π or δ binding between sulfur and ruthenium. Because the effective metal orbitals lie in mirror planes and there must be nonzero orbital coefficients on the intervening atoms to allow electron transfer to occur, the "transferred" electron must occupy an even orbital with respect to these planes. A d_{z^2} like orbital, for example, would suffice. Nonzero coefficients in both planes are required by the form of our Hamiltonian and the assumption of only nearest-neighbor interaction. This restriction causes the following sets of orbitals (shown in Figure 1) to have equal amplititude: $\{\phi_{1a},\phi_{1b}\}$, $\{\phi_{2a},\phi_{2b}\}$, $\{\phi_{3a},\phi_{3b}\}$, $\{\phi_{4a},\phi_{4b}\}$, $\{\phi_{5a}, \phi_{5b}, \phi_{5c}, \phi_{5d}\}$, $\{\phi_{6a}, \phi_{6b}, \phi_{6c}, \phi_{6d}\}$. Because of the symmetry, there are only six unique basis functions per unit cell. The complete 16-orbital and symmetrized 6-orbital unit cells are shown in Figure 1. The wave function is assumed to be of the form (according to the above recipe)

$$\psi = \sum_j [(a\phi_1 + b\phi_2 + c\phi_3 + d\phi_4 + f\phi_5 + g\phi_6)\epsilon^j + W(a\phi_2 + b\phi_1 + c\phi_4 + d\phi_3 + f\phi_5 + g\phi_6)\epsilon^{N-j}] + \lambda\phi_L + \Omega\phi_R \quad (6)$$

where ϕ_1 is the symmetric combination of ϕ_{1a} and ϕ_{1b}, etc. For the central region of the molecule there are three exchange parameters and one Coulomb interaction parameter (α): β, γ, β_{CH}, and α_H. Figure 1a shows the interactions related to these parameters. The carbon sp^3 Coulomb energy is chosen as the energy zero. Zero overlap is assumed between orbitals on neighboring atoms. The special relationship between the energy and the decay constant, ϵ, holds in the infinite spiroalkane as well as in the mixed-valence dithiaspiro complexes. It is determined by integrating the Schrödinger equation for the infinite spiroalkane over the six symmetrized orbitals in the unit cell. Other unit cell choices are possible and should give identical wave functions.

One integrates the Schrödinger equation for the infinite chain ($W = 0$, $\lambda = 0$, $\Omega = 0$ in eq 6) or the finite problem. Assuming zero overlap the matrix equation (eq 7) must hold. The determinant of the matrix must equal zero. This gives the energy–ϵ relationship that is carried into the finite problem due to the

$$\begin{bmatrix} -E & \gamma & 0 & \beta & 2\gamma & 0 \\ \gamma & -E & \beta & 0 & 2\gamma & 0 \\ 0 & \beta & \gamma - E & 2\gamma\epsilon & 0 & 0 \\ \beta & 0 & 2\gamma/\epsilon & \gamma - E & 0 & 0 \\ \gamma & \gamma & 0 & 0 & \gamma - E & \beta_{CH} \\ 0 & 0 & 0 & 0 & \beta_{CH} & \alpha_H - E \end{bmatrix} \begin{bmatrix} a \\ b \\ c \\ d \\ f \\ g \end{bmatrix} = 0 \quad (7)$$

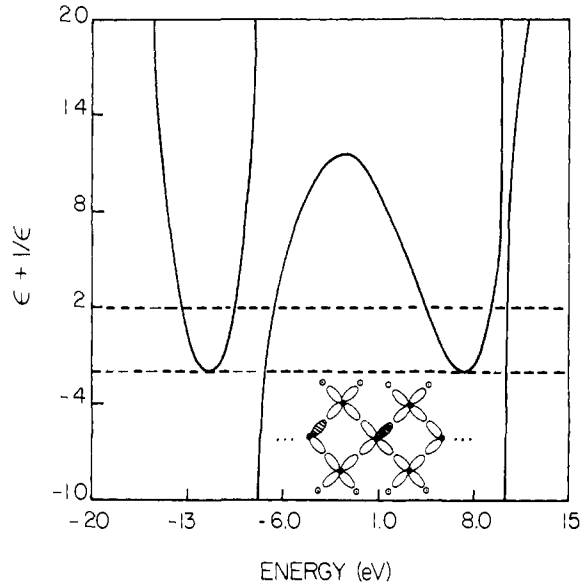

Figure 2. This shows the ($\epsilon + 1/\epsilon$) dependence on E resulting from eq 7. The band gap falls between −6.6 and +4.2 eV. The eigenstates of the infinite problem fall between the dashed lines.

(27) Richardson, D. E.; Taube, H. *J. Am. Chem. Soc.* **1983**, *105*, 40–51.
(28) McConnell, H. M. *J. Chem. Phys.* **1961**, *35*, 508–515.
(29) Morton-Blake, D. A. *Theor. Chim. Acta* **1979**, *51*, 85–95; **1980**, *56*, 93–112; **1981**, *59*, 213–227; **1982**, *61*, 193–202.
(30) Koiller, B.; Brandi, H. S. *Theor. Chim. Acta* **1981**, *60*, 11–17.
(31) Brandi, H. S.; Koiller, B.; Ferreira, R. *Theor. Chim. Acta* **1981**, *60*, 89–96.
(32) Larsson, S. *Discuss. Faraday Soc.* **1982** *74*, 390–392.
(33) Ashcroft, N. W.; Mermin, N. D. "Solid State Physics"; Saunders: Philadelphia, 1976; Chapters 8, 10, and 28.
(34) Taylor, P. L. "A Quantum Approach to the Solid State"; Prentice Hall: Englewood Cliffs, N.J., 1970; Chapter 2.

periodic potential in the molecule's central region. Neighboring unit cells only communicate with other cells via orbitals 3 and 4. Therefore, factors of ϵ and $1/\epsilon$ appear in eq 7 only once. It is useful to write this equation in the form $(\epsilon + 1/\epsilon) = x(E)/y(E)$. $x(E)$ is a sixth degree polynomial. $y(E)$ is a second degree polynomial. $x(E)$ arises from the carbon backbone. The C–H bonds split the energies associated with the backbone, giving rise to the second degree $y(E)$. A plot of this equation is shown in Figure 2 for specific choices of the parameters. Points on these curves correspond to eigenstates for molecules containing spiroalkane unit cells. The exact positions of the allowed states for a given problem are determined by the boundary conditions imposed on the linker. ϵ may have real and imaginary parts. Delocalized states (Bloch states) correspond to $\epsilon = \exp(i\vec{k}\cdot\vec{R})$ and $|\epsilon| = 1$.[35] These are the states between the dashed lines (± 2) and correspond to allowed energies for the one-dimensional "crystal" comprised of spiroalkane unit cells. Other states ($|\epsilon| < 1$) correspond to localized states.

One must select Coulomb and exchange parameters corresponding to the traditional extended-Hückel parameters. Because we are interested in carbon interactions in periodic networks, we use the tight-binding parameters fit to diamond structure calculations which in turn fit the known band structure and optical properties of diamond.[36] We are interested first in getting the E–ϵ relationship of the system correct rather than calculating experimental energies. Toward this end the diamond paameters are more appropriate than the standard extended Hückel parameters. In this calculation carbon sp^3 hybrid orbitals are chosen as the carbon basis orbitals. It is never necessary to explicitly write these orbitals in terms of Slater or Gaussian functions because the interaction parameters are available from the diamond calculation.[37]

A form of the extended-Hückel exchange parameter in general use is [38,39]

$$H_{ab} = K(E_a + E_b)S/2 \qquad (8)$$

K is set by the theorist, E_a and E_b are orbital ionization energies, and S is the overlap between atomic orbitals. If E_a and E_b are the orbital ionization energies of sp^3 carbon orbitals (available from tables) and $S \simeq 0.65$, then $K = 1.0$ to fit the diamond parameters to eq 8.[40,41] The orbital ionization energy of hydrogen compared to a carbon 2s orbital is 5.9 eV based on the standard tables.[40] $\gamma = {}^1/_4(\alpha_S - \alpha_P)$. From the diamond calculation, the sp^3 Coulomb energy of carbon is 5.55 eV relative to carbon 2s. The carbon sp^3 Coulomb integral was chosen as the energy zero. Hence, α_H is 0.35 eV. A carbon–hydrogen overlap of 0.69, Coulomb energies from the orbital ionization energy tables, and the above K factor gives $\beta_{CH} = -9.14$ eV.[39,40] These values were used in eq 7 to generate Figure 2. The orbital interactions are summarized in Table I.

Boundary Conditions. Now that the energy–decay constant relationship is determined for the spiroalkane linker, we must find where on Figure 2 the ruthenium localized states appear. The infinite spiroalkane has a band gap from −6.7 to +4.4 eV. Calculations of the solid-state properties of crystalline materials containing impurities suggest that localized states will occur in the gap regions.[30–33] Just where these states occur and what their decay constant is depend critically on how we choose the terminal orbitals. We model each metal–pentaammine with a single effective orbital. The important Ru effective orbital must be even with respect to reflection through the two mirror planes which include the metals. Sulfur–ruthenium interactions are probably mediated by several orbitals.[9,42–45] It is known that the carbon–sulfur–carbon bond angle in the spiro ring is ~78°.[46] Strained bonds such as these prefer an increased p electron content. Yet, for this model we choose to place sp^2 orbitals on the sulfur. This provides ruthenium with an orbital even with respect to the two mirror planes with which to interact. One might have chosen more complex combinations of orbitals. The energy–ϵ relationship shown in Figure 2, however, is independent of these choices. The choice of sulfur orbitals weakly contributes to the position on the plot where the localized states fall. The most critical parameters are the metal Coulomb energies. The sulfur parameters are shown in Table II. They were obtained for sp^2 orbitals using $K = 1.0$, $S_{SC} = 0.37$, and the same orbital ionization energy table.[40,41]

Table I. C and H Parameter Values

parameter	energy (eV)
β	−8.47
γ	−1.85
β_{CH}	−9.14
α_H	0.35
$\alpha_C(sp^3)$	0.00

Table II. Sulfur Parameter Values

parameter	energy (eV)
β_{SC}	−5.11
γ_S	−3.00
α_S	−0.75

One now integrates the Schrödinger equation over the six unique boundary orbitals and their nearest neighbors. Simultaneously satisfying these equations (eq 9) and the energy–ϵ equation (eq 7) determines the eigenvalues and eigenfunctions of the system. The first four lines in the determinant result from integrating the Schrödinger equation over the orbitals near Ru(II). The last four lines result from the orbitals near Ru(III). In eq 9 $b' = b/a$ and $f' = f/a$, where b and a represent the coefficients in eq 6. The effective metal–sulfur resonance integrals, β_{3S} and β_{2S}, were calculated by the method of Harrison and Froyen.[47,48] We find $\beta_{2S} = -2.14$ eV and $\beta_{3S} = -1.57$ eV. The Coulomb energies of the two effective ruthenium orbitals were determined uniquely based on two requirements. First, the energy of the intervalence charge-transfer band must match the experimental energy. Second, the energy of the sulfur to Ru(III) ligand to metal charge-transfer band (LMCT) must match the experimental energy. For the mixed-valence molecules these LMCT energies are 2.74, 2.68, and 2.70 eV for the two-, three-, and four-ring systems. The two "effective" metal pentaammine orbitals each represent 21 atoms by only one orbital. Therefore, the actual Coulomb energy (α_2 or α_3) of this "orbital" is not, of itself, physically meaningful.

With these assumptions the wave functions are uniquely determined for I, II, and III. Computationally, we examined a large number of energies, calculated ϵ from eq 7, and evaluated the determinant in eq 9. For each energy these are two roots of ϵ. By convention we choose the value of ϵ less than 1. The energy of the highest occupied bridge state was determined from an extended-Hückel calculation on the two- and three-ring mixed-valence compounds to be about −7.0 eV. This energy was assumed to remain the same for the four-ring system.

The tunneling matrix element is calculated from the dipole matrix element (eq 2). We calculated the two metal localized wave functions of the system in the band gap and approximated

(35) $\vec{k}$ is a purely real vector in this case.
(36) Chadi, D. J.; Cohen, M. L. *Phys. Status Solidi, B* **1975**, *68*, 405–419.
(37) One could also have used the work of footnotes 2 and 13 in Chadi and Cohen's work (ref 36 in this paper).
(38) Daudel, R.; Sandorfy, C. "Semiempirical Wave-mechanical Calculations on Polyatomic Molecules"; Yale University Press: New Haven, 1971.
(39) Yates, K. "Hückel Molecular Orbital Theory"; Academic Press: New York, 1978.
(40) Ballhausen, C. J.; Gray, H. B. "Molecular Orbital Theory"; Benjamin/Cummings: London, 1964; p 122.
(41) Mulliken, R. S. *J. Am. Chem. Soc.* **1950**, *72*, 4493–4503.
(42) Kuehn, C. G.; Taube, H. *J. Am. Chem. Soc.* **1976**, *98*, 689–702.
(43) Stein, C. A.; Taube, H. *J. Am. Chem. Soc.* **1978**, *100*, 1635–1637.
(44) Stein, C. A.; Taube, H. *Inorg. Chem.* **1979**, *18*, 1168–1170.
(45) Stein, C. A.; Taube, H. *Inorg. Chem.* **1979**, *18*, 2212–2216.
(46) Tagaki, W. In "Organic Chemistry of Sulfur"; Oae, S., Ed.; Plenum: New York, 1977; p 247.
(47) Harrison, W. A.; Froyen, S. *Phys. Rev. B* **1980**, *21*, 3214–3221.
(48) Froyen, S. *Phys. Rev. B* **1980**, *22*, 3119–3121.

$$\det \begin{bmatrix} \alpha_2 - E & \beta_2 S & 0 & 0 & 0 & 0 & 0 & 0 \\ \beta_2 S & \alpha_S - E & 2\gamma_S & 0 & 0 & 0 & 0 & 0 \\ 0 & \gamma_S & \gamma_S + \alpha_S - E & \beta_{SC}\epsilon & \beta_{SC}\epsilon^N b' & 0 & 0 & 0 \\ 0 & 0 & \beta_{SC} & (2\gamma f'\epsilon + \gamma b'\epsilon - E\epsilon) & (2\gamma f'\epsilon^N + \gamma\epsilon^N - Eb'\epsilon^N) & 0 & 0 & 0 \\ 0 & 0 & 0 & (2\gamma f'\epsilon^N + \gamma\epsilon^N - Eb'\epsilon^N) & (2\gamma f'\epsilon + \gamma b'\epsilon - E\epsilon) & \beta_{SC} & 0 & 0 \\ 0 & 0 & 0 & \beta_{SC} b'\epsilon^N & \beta_{SC}\epsilon & \gamma_S - E + \alpha_S & \gamma_S & 0 \\ 0 & 0 & 0 & 0 & 0 & 2\gamma_S & \alpha_S - E & \beta_3 S \\ 0 & 0 & 0 & 0 & 0 & 0 & \beta_3 S & \alpha_3 - E \end{bmatrix} \quad (9)$$

the dipole matrix element between these states with the formula

$$\langle \psi_g | e\vec{x} | \psi_{ex} \rangle \simeq e \sum_i C_{g_i}^* C_{ex_i} X_i \quad (10)$$

where $C_{g_i}^*$ = coefficient of ith ground-state atomic orbital, C_{ex_i} = coefficient of ith excited-state atomic orbital, and $X_i = X$ coordinate of ith atom. This formula is reliable to the extent that orbital overlap is small and the x coordinate changes slowly as one moves between metal atoms.[49-52] The dipole matrix element involves only the position along the axis joining the metal atoms. The y and z components of the matrix element cancel because of the inversion symmetry of the four-member rings. In eq 1 and 2 a is the through-space distance.

Though semiempirical in approach, this adapted tight-binding method for calculating localized states in mixed-valence molecules offers many benefits. A fairly simple calculation allows the prediction of the rate of decay (ϵ) of a localized wave function with distance as a function of redox energy. The band-structure determination is not complicated. Even simple models of n-alkane and spiroalkane produce ϵ–E relationships in the gap region (see Figure 3a and 3b) very similar to the more complex models. We are able to separate the calculation of the tunneling matrix elements into two parts. First the band structure of the rigid bridge is determined. This structure sets limits on the decay of the wave function with distance. Second we impose boundary conditions on the problem dependent on the redox properties of the electron donor and acceptor. Together these properties determine the electronic tunneling matrix element. The band structures for several other unit cell choices are shown in Figures 4a–d. The validity of the form of the wave function in eq 6 was confirmed by finding the eigenvalues and eigenvectors of the full extended-Hückel problem (a 16 × 16 matrix in the case of the two-ring system). For the two-ring system the wave functions found by the two approaches were consistent.

In the case of long-distance electron transfer between well-localized states, the wave functions may be approximated. For an arbitrary unit cell the two localized wave functions are given approximately by

$$\psi_g \simeq \omega\phi_0 + \epsilon_1\phi_1 + \epsilon_1^2\phi_2 + \ldots + \epsilon_1^{N-1}\phi_{N-1} + \epsilon_1^N\phi_N + \zeta\phi_{N+1}$$

and

$$\psi_{ex} \simeq \delta\phi_0 + \epsilon_2^N\phi_1 + \epsilon_2^{N-1}\phi_2 + \ldots + \epsilon_2^2\phi_{N-1} + \epsilon_2\phi_N + \eta\phi_{N+1}$$

For the optical problem at hand $\epsilon_1 > \epsilon_2$ because the ground state is closer to the bonding states than the excited states (both are very far from the antibonding states); $0 < \epsilon < 1$, $\delta \simeq 0$, and $\zeta \simeq 0$. The optical tunneling matrix element between the localized states is

$$T_{ab}^{op} \simeq (\sum_i X_i A_i^g B_i^{ex})\Delta E/a \simeq (\Delta X/a)(\Delta E)\epsilon_2\epsilon_1^N \propto \epsilon_2\epsilon_1^N \quad (11a)$$

N is the number of atoms in the linker backbone, and we have ignored all terms in ϵ_2^j for $j > 1$. A_i and B_i are orbital coefficients. ϵ_1 and ϵ_2 represent the wave-function decay per unit cell but may be converted to the decay per carbon atom. In the thermal electron-transfer reactions, $\epsilon_1 = \epsilon_2$ in the activated complex (by energy conservation). Rather than relating the thermal matrix element to a splitting between even and odd electronic states (see later section), we may use the above zeroth-order wave functions (when $\delta = \zeta = 0$) to calculate the electronic Hamiltonian matrix element between the states. In the thermal-transfer problem $E_g = E_{ex}$, $\epsilon_1 = \epsilon_2$, $\eta = \omega$, $\zeta = \delta$, and the part of the Hamiltonian omitted in writing ψ_g is $H' = (a_{N+1}^+ a_N + a_N^+ a_{N+1})\beta'$.

$$\langle \psi_g | H' | \psi_{ex} \rangle = \beta'\eta\epsilon^N \quad (11b)$$

$$T_{ab}^{th} \propto \epsilon^N$$

Thus, addition of an extra unit cell to the linker changes the donor–acceptor matrix element by approximately a factor of ϵ. Tables VI and VII verify that these simple arguments are valid for the spiro molecules. The thermal tunneling matrix element is frequently expressed as

$$T_{ab} \simeq A \exp(-\alpha R) \quad (12)$$

for long-distance charge transfer. ϵ is simply related to α. R is

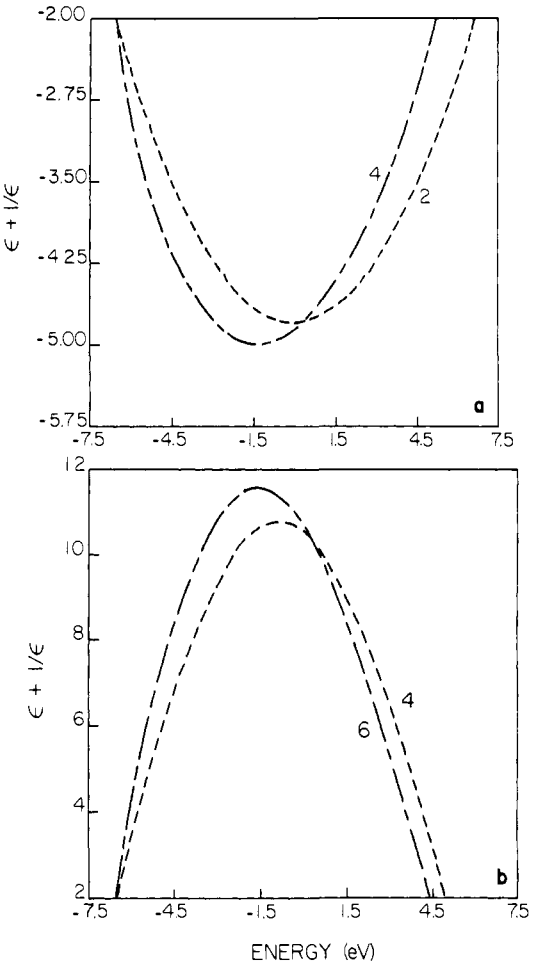

Figure 3. (a) The $\epsilon + 1/\epsilon$ dependence on energy for a two orbital per site n-alkane model (marked 2) and the full four symmetrized orbital per site n-alkane (marked 4) is shown. Parameters are taken from Table I. The two orbital per site model makes relatively good predictions of $\epsilon + 1/\epsilon$. (b) As in (a), comparing the full six symmetrized orbitals per unit cell spiroalkane (marked 6) with the four symmetrized orbital per unit cell (no C–H bonds) spiroalkane (marked 4). Parameters are taken from Table I.

(49) Robin, M. B.; Day, P. *Adv. Inorg. Chem. Radiochem.* **1967**, *10*, 247–422.
(50) Mulliken, R. S. *J. Chem. Phys.* **1939**, *7*, 14–20, 20–34.
(51) Mulliken, R. S.; Person, W. B. "Molecular Complexes"; Wiley: New York, 1969.
(52) Hoijtink, G. J. In "Molecular Orbitals in Chemistry, Physics, and Biology"; Academic Press: New York, 1964.

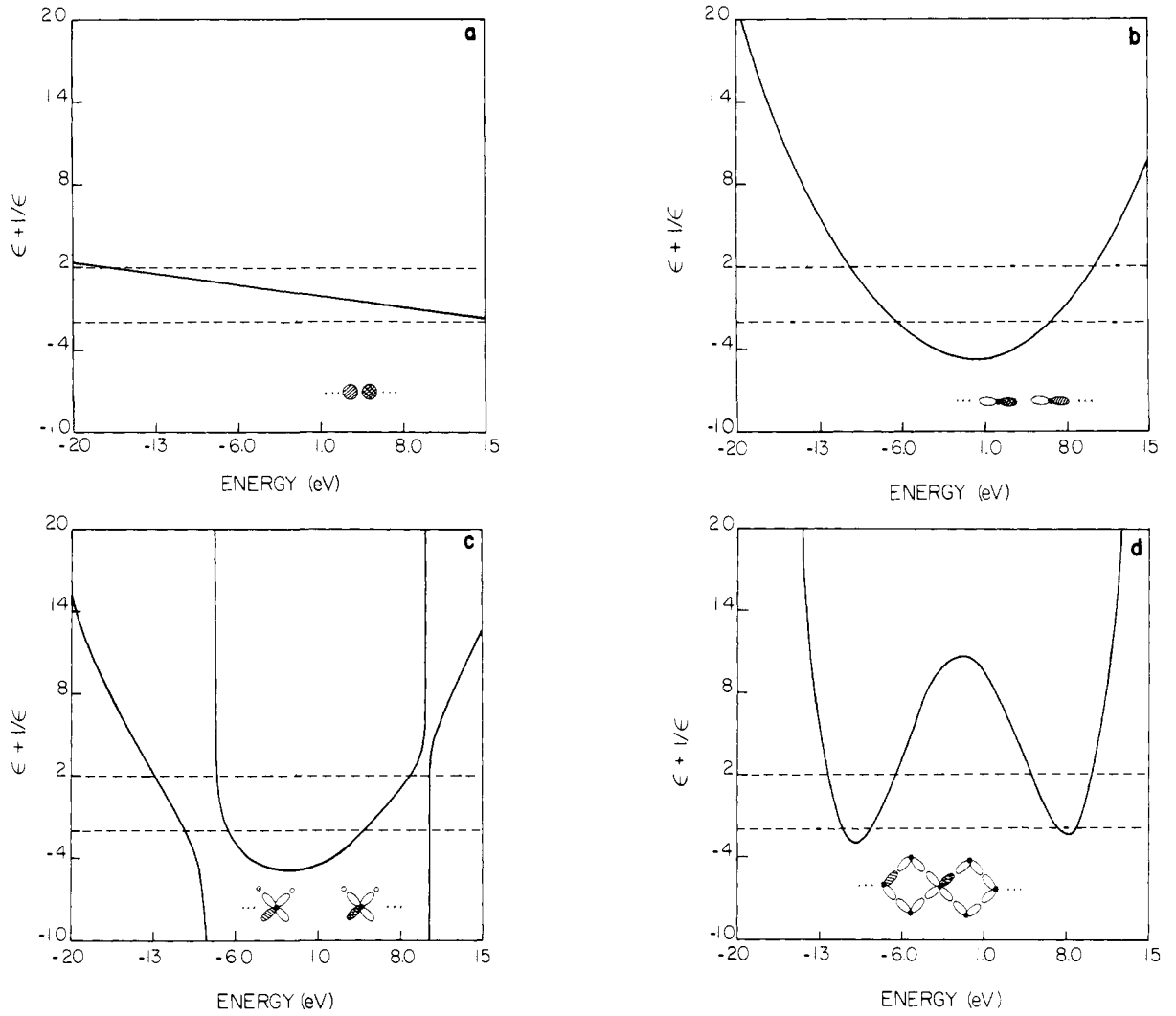

Figure 4. Band structures for several units cell choices are shown. Interaction parameters are chosen from Table I. $\epsilon + 1/\epsilon = \pm 2$ is marked with dashed lines. (a) The one orbital per site model. (b) The two orbital per site model. (c) The four symmetrized orbital per site *n*-alkane model. (d) The four symmetrized orbital per site model of spiroalkane. Shaded orbitals indicate corresponding orbitals of adjacent unit cells.

Table III. Comparison of Decay Constants ϵ and α

unit cell	distance measured through[a]	carbon atoms traversed	α (Å^{-1})
n-alkane	bond	1	$-(\ln \epsilon)/1.54$
n-alkane	space	2	$-(\ln \epsilon)/2.4$
spiroalkane	bond	2	$-(\ln \epsilon)/3.08$
spiroalkane	space	2	$-(\ln \epsilon)/2.22$

[a] Through-space distance is the shorted distance between ends of a "taut" molecule. All calculations assume bond-mediated transfer. Through-space distances are given for comparison although the transfer is still calculated through bond.

sometimes chosen as a through-bond distance and sometimes as a through-space distance. Table III shows the expressions relating α to ϵ for spiroalkane and *n*-alkane for both through-bond and through-space distance measurements. The actual calculations on the spiroalkanes do not use the approximation of eq 11a and 11b.

Comparison with Experiment

Photoassisted Charge Transfer. Varying the end orbital parameters for fixed metal–sulfur interaction parameters we found metal localized states in the band gap region of Figure 2. We varied the Coulomb integrals of Ru(III) and Ru(II) to fit the energy of the intervalence charge-transfer band and the ligand to Ru(III) charge-transfer band. The localized states are very near the valence band. This result suggests that, in these molecules, charge transfer is mediated by hole transfer through the bonding states of the linker. The energies, decay constants, and Coulomb parameters resulting from the fit are given in Table IV. The dipole matrix elements were calculated with eq 2 assuming a distance of 1.11 Å between all nonmetal nuclei (measured along the metal–metal axis). The metal–sulfur distances were taken from ref 3. The calculation of $|T_{ab}|$ from experiment (ref 3) assumed the appropriate distance to be used in eq 1 was the through-bond distance. In the optical charge-transfer formalism, however, the through-space distance is required when calculating with eq 1 and 2. Corrected values of $|T_{ab}|$ determined from the

Table IV. Calculated Optical Tunneling Matrix Elements[a]

no. of rings	α_2	α_3	E_g	ϵ_g	E_{ex}	ϵ_{ex}	$\langle\psi_g\|\vec{x}\|\psi_{ex}\rangle$	T_{ab}
2	−5.4	−4.0	−5.7	0.20	−4.3	0.11	-4.9×10^{-2}	-7.2×10^{-3}
3	−5.6	−4.0	−5.9	0.22	−4.3	0.11	-1.0×10^{-2}	-1.3×10^{-3}
4	−5.9	−4.0	−6.1	0.27	−4.3	0.11	-3.1×10^{-3}	-4.1×10^{-4}
5	−5.9	−4.0	−6.1	0.27	−4.3	0.11	-8.4×10^{-4}	-9.5×10^{-5}
6	−5.9	−4.0	−6.1	0.27	−4.3	0.11	-2.3×10^{-4}	-2.3×10^{-5}

[a] Position matrix element in Å; all other values are eV.

Table V. Corrected Experimental T_{ab}'s

no. of rings	E^{op} (eV)	metal–metal through-space distance (Å)	$\|T_{ab}\|$ (eV)
2	1.36	9.3	2.1×10^{-2}
3	1.54	11.5	8.5×10^{-3}
4	1.80	13.7	4.0×10^{-3}

experiments are given in Table V.

The comproportionation constants for these molecules are not known. Since no separation was observed between the two waves in the cyclic voltammetry experiments, it is reasonable to assume that the metals are oxidized in a statistical fashion with $K_{com} = 4$.[27] If the metals were oxidized in a statistical fashion with no regard for the oxidation state of the other end of the molecule, the assumed concentrations of mixed-valence species would be a factor of 2 too large. The calculated values for $\mathbf{T}_{ab}$, in turn, would be too small by the factor $(1/\sqrt{2})$. The experimentally determined $|T_{ab}|$ is roughly 0.62 exp(−0.37R), where R is the through-space metal–metal distance in Å.

Both the magnitude and decay of the calculated $\mathbf{T}_{ab}$ fit the experimentally determined values fairly well with respect to decay length and prefactor (eq 12). $\mathbf{T}_{ab}$ for the four-ring system is calculated to be 0.31 of the three-ring value. The change corresponds to a through-space α of 0.53 Å^{-1}. The calculated through-space prefactor (A) for the four-ring system is −0.58 eV. The average change of $\mathbf{T}_{ab}$ upon addition of a unit cell is a factor of 0.25; thus the average through-space calculated α is found to be ~0.63. This calculation can be performed for an arbitrary number of linkers. $\mathbf{T}_{ab}$ is predicted for the five- and six-ring systems (see Table IV).

The value ϵ in spiroalkane is roughly the factor by which the wave function decays upon moving between any two corresponding orbitals in adjacent unit cells. In the case of spiroalkane there are two carbon atoms between the corresponding carbon orbitals on adjacent unit cells. For the purpose of comparing wave-function decays per *carbon atom*, we define $\epsilon' = \epsilon^{1/2}$. Thus, a mostly localized electron mixing weakly with a spiroalkane chain has an amplitude which decays by a factor of ϵ' per carbon atom in the spiro backbone. Seitz and Taube report an exinction coefficient of 5 M^{-1} cm^{-1} for IV.[2] This is a nonrigid molecule, but since

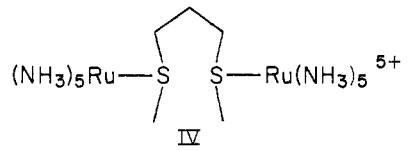

IV

the intervalence band extinction coefficient is so small and the Coulombic repulsion between metals favors a large through-space ruthenium distance, it is likely that direct Ru–Ru through-space interactions are small. The extinction coefficient varies as the square of the tunneling matrix element. According to eq 11a $\mathbf{T}$(alkane)/$\mathbf{T}$(spiro) ≃ (0.25/0.33)(0.33/0.45)^N. Thus $\mathbf{T}^2$(alkane)/$\mathbf{T}^2$(spiro) ≃ 0.17. Hence, the extinction coefficient for IV is expected to be (0.17)(43) or 7.3 M^{-1} cm^{-1}, very close to the experimental value. The values of ϵ used here are decay per carbon atom (ϵ') and are taken from Table IV and Figure 5b. N equals 2. Figures 5a and 5b compare n-alkane and spiroalkane in the band gap region.

Predictions for Related Experiments. Taube and Stein have prepared the mixed-valence *trans*-isnoctaammine complex of the two-ring ligand (isn = isonicotinamide). Little change in extinction coefficient was found. Since there is a fair amount of uncertainty in the choice of the sulfur–metal interactions in our method, we can best compare the *decrease* of T_{ab} *with distance* for different redox energy electron traps. It is harder to calculate the exact change in rate for a fixed number of rings due to ligand or metal substitution because such changes effect the boundary conditions in subtle ways. The redox potential of $Ru(NH_3)_4$isn is changed by +0.2 V compared to $Ru(NH_3)_5$ in the spiro molecules.[2] Changing α_3 and α_2 by −0.2 eV from their values in Table IV causes $\langle\psi_g|\vec{x}|\psi_{ex}\rangle$ to change by a factor of 0.23 in going from two

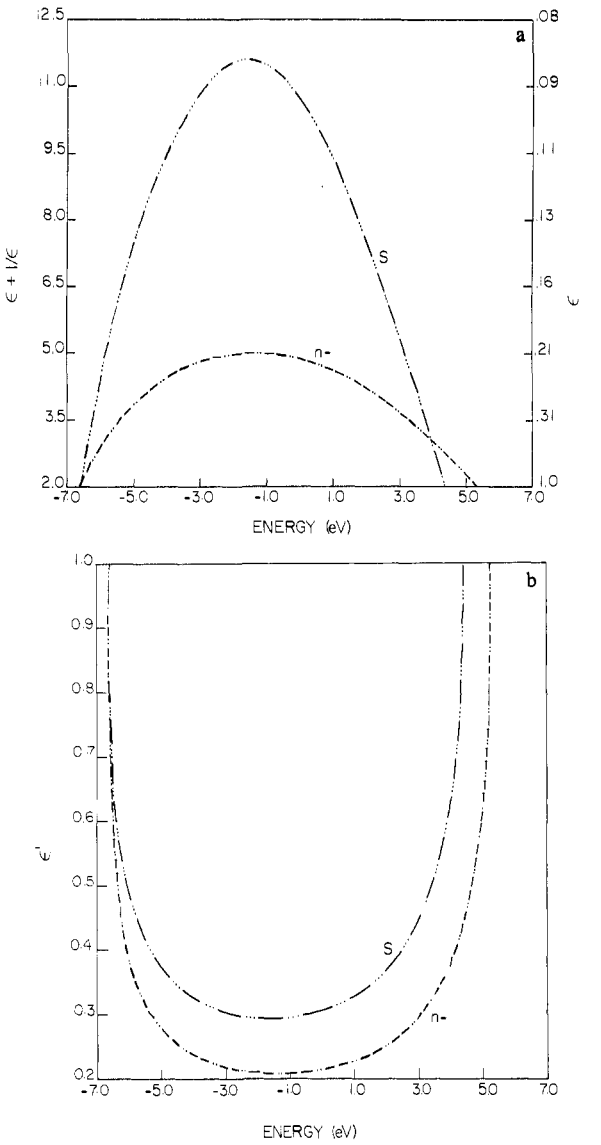

Figure 5. (a) The $\epsilon + 1/\epsilon$ dependence on energy for n- and spiroalkanes is shown. The sign of $\epsilon + 1/\epsilon$ for n-alkane is reversed from its true value. The horizontal line represents the edge of the band gap. The parameters were chosen from Table I. Figure 6b can be obtained from this by solving a quadratic in ϵ. (b) The ϵ' (decay per carbon atom) dependence on electron energy for spiro- and n-alkanes in the band gap. The decay constant for spiro- is everywhere greater than for the n-alkane. Parameters are taken from Table I. In both figures "S" marks the spiroalkane curves and "n-" the n-alkane curves.

to three rings. $\mathbf{T}_{ab}$ according to eq 2, is predicted to change by a factor of 0.21 on going from the two-ring isn to the three-ring isn system. The pentaammine system was calculated to change T_{ab} by a factor of 0.15 on going from the two- to three-ring system. A smaller distance from the valence band was indeed expected to make the isn-localized state wave functions decay more slowly compared to the pentaammine states.

Our method allows the prediction of the effect of altered electron donor and acceptor trap depth (redox energy) on ϵ and hence on $\mathbf{T}_{ab}^{op}$. We give several illustrations for the spiroalkane system where the Coulomb energies of the metals are both changed. Such a change might be induced by ligand or metal substitution, or by a change of solvent. The values of the parameters, energies of the localized states, and the tunneling matrix elements are given in Table VI. Changing the redox levels of the electron traps alters the decay of T_{ab} with distance. This decay constant is, therefore, not a "universal" parameter. Because of uncertainties in β(S–Ru), direct comparison of $\langle\psi_g|\vec{x}|\psi_{ex}\rangle$ for different redox levels but constant number of rings is discouraged.

Thermally activated electron exchange may also be an im-

Table VI. Optical T_{ab} for Altered Trap Depths[a]

no. of rings	α_3	α_2	E_g	ϵ_g	E_{ex}	ϵ_{ex}	$\langle\psi_g\vert\vec{x}\vert\psi_{ex}\rangle$	T_{ab}
2	−4.9	−3.4	−5.3	0.16	−3.8	0.10	-4.4×10^{-2}	-7.1×10^{-3}
3	−4.9	−3.4	−5.3	0.16	−3.8	0.10	-7.4×10^{-3}	-9.7×10^{-4}
4	−4.9	−3.4	−5.3	0.16	−3.8	0.10	-1.2×10^{-3}	-1.3×10^{-4}
2[b]	−5.6	−4.2	−5.9	0.22	−4.5	0.12	-5.2×10^{-2}	-7.8×10^{-3}
3	−5.8	−4.2	−6.0	0.25	−4.5	0.12	-1.2×10^{-2}	-1.6×10^{-3}
4	−6.1	−4.2	−6.3	0.33	−4.5	0.12	-4.9×10^{-3}	-6.4×10^{-4}
2	−6.3	−4.8	−6.4	0.43	−5.0	0.14	-7.0×10^{-2}	-1.1×10^{-2}
3	−6.3	−4.8	−6.4	0.43	−5.0	0.14	-2.8×10^{-2}	-3.4×10^{-3}
4	−6.3	−4.8	−6.4	0.43	−5.0	0.14	-1.2×10^{-2}	-1.2×10^{-3}
2	−6.5	−5.0	−6.6	0.72	−5.2	0.15	-8.6×10^{-2}	-1.2×10^{-2}
3	−6.5	−5.0	−6.6	0.69	−5.2	0.15	-4.7×10^{-2}	-5.7×10^{-3}
4	−6.5	−5.0	−6.6	0.68	−5.2	0.15	-2.9×10^{-2}	-3.0×10^{-3}

[a] $\beta_{2S} = -2.14$, $\beta_{3S} = -1.57$, all energies in eV. [b] The second set of values corresponds roughly to the isn analogues of the pentaammine mixed-valence complexes.

Table VII

no. of rings	$\alpha_3 = \alpha_2$	E_b	ϵ_b	E_a	ϵ_a	T_{ab}
	A. Calculated Thermal Tunneling Matrix Elements[a]					
2	−4.7	−5.06	0.14	−5.04	0.14	7.5×10^{-3}
3	−4.8	−5.14	0.15	−5.14	0.15	1.1×10^{-3}
4	−4.95	−5.27	0.15	−5.27	0.15	1.8×10^{-4}
5	−4.95	−5.27	0.15	−5.27	0.15	2.8×10^{-5}
	B. Thermal T_{ab} for Altered Trap Depths[b]					
2	−4.2	−4.6	0.12	−4.6	0.12	7.3×10^{-3}
3	−4.2	−4.6	0.12	−4.6	0.12	9.1×10^{-4}
4	−4.2	−4.6	0.12	−4.6	0.12	1.1×10^{-4}
2[c]	−4.9	−5.2	0.15	−5.2	0.15	7.7×10^{-3}
3	−5.0	−5.3	0.16	−5.3	0.16	1.2×10^{-3}
4	−5.15	−5.4	0.17	−5.4	0.17	2.2×10^{-4}
2	−5.5	−5.8	0.20	−5.7	0.20	9.1×10^{-3}
3	−5.5	−5.7	0.20	−5.7	0.20	1.8×10^{-3}
4	−5.5	−5.7	0.20	−5.7	0.20	3.5×10^{-4}
2	−6.4	−6.5	0.50	−6.5	0.50	1.7×10^{-2}
3	−6.4	−6.5	0.50	−6.5	0.50	7.8×10^{-3}
4	−6.4	−6.5	0.50	−6.5	0.50	3.7×10^{-3}

[a] $\beta_{3S} = \beta_{2S} = -1.86$; $T_{ab} = {}^1/_2(E_a - E_b)$; all energies in eV. [b] $\beta_{3S} = \beta_{2S} = -1.86$, all energies in eV. [c] The second set of values corresponds roughly to the isn analogues of the pentaammine mixed-valence complexes.

portant process in these mixed-valence molecules. The thermal electron-tunneling matrix element is just half the symmetric antisymmetric splitting when $\alpha_3 = \alpha_2$ and $\beta_{2S} = \beta_{3S}$. Choosing these parameters to be equal to the averages of the parameters used in the optical charge-transfer process yields predictions of the thermal tunneling matrix elements for the pentaammine complexes (Table VIIA).[53] We find the distance dependence of T_{ab} to be similar to the distance dependence found for the optical process. Table VIIB shows the energy splitting for $\alpha_3 = \alpha_2$ and $\beta_{2S} = \beta_{3S} = -1.86$ at several points in the band gap.

For the case corresponding roughly to isn-substituted systems ($\alpha_3 = \alpha_2 = -4.9$ eV, $\beta_{3S} = \beta_{2S} = -1.86$ eV, two rings), $T_{ab} = 7.7 \times 10^{-3}$ eV. For three rings $\alpha_3 = \alpha_2 = -5.0$ eV, $\beta_{3S} = \beta_{2S} = -1.86$ eV, and $T_{ab} = 1.2 \times 10^{-3}$ eV. T_{ab} (thermal) has changed by a factor of only ~0.16. Compare this to the values in Table VA (~0.15) per linker cell). More drastic effects will be seen on the thermal matrix element by *considerably* changing the redox level of the coordinated metals.

General Discussion

Geometric Effects on T_{ab}. The considerable difference in electron mediation properties of *n*-alkane compared to spiroalkane linker arises from the two equivalent electronic pathways in each unit cell of spiroalkane. In the spiro molecules the electrons have twice the number of transfer routes, and the wave function amplitude essentially adds at each quaternary center before decaying into the next ring.

The energy–ϵ relationship for an *n*-alkane where the carbon orbtials are represented by a single orbital and there are two atoms per unit cell is

(53) This argument is justified by electron-hole symmetry.

Table VIII. Comparison of Decay Constants for Spiro- and *n*-Alkane[a]

energy, (eV)	alkane		spiroalkane		
	$\epsilon + 1/\epsilon$	$\vert\epsilon\vert$	$\epsilon + 1/\epsilon$	$\vert\epsilon\vert$	$\vert\epsilon'\vert$
4.0	−3.0	0.38	2.9	0.40	0.63
3.0	−3.7	0.30	5.3	0.20	0.44
2.0	−4.2	0.25	7.5	0.14	0.40
1.0	−4.6	0.23	9.4	0.11	0.33
0.0	−4.9	0.22	10.7	0.09	0.31
−1.0	−5.0	0.21	11.5	0.09	0.30
−2.0	−5.0	0.21	11.5	0.09	0.30
−3.0	−4.8	0.22	10.9	0.09	0.30
−4.0	−4.4	0.23	9.4	0.11	0.33
−5.0	−3.9	0.28	7.3	0.14	0.37
−6.0	−2.9	0.39	4.4	0.24	0.48

[a] ϵ is the decay per unit cell. ϵ' is the decay per carbon atom.

$$(\epsilon + 1/\epsilon) = E^2/\beta^2 - 2$$

For spiroalkane represented with one orbital per carbon atom

$$(\epsilon + 1/\epsilon) = (E^2/2\beta^2) - 2$$

and there are three atoms per unit cell (this equation results from the case even with respect to the mirror planes). Hydrogen atoms were ignored in both cases. We see that the spiro linkage is equivalent to replacing β in the linear problem with $\sqrt{2}\beta$. The thermal matrix element in the one orbital per atom linear problem is proportional to $(\beta/\Delta)^N$, where β is the exchange integral, Δ is energy of the electron traps, and N is the number of unit cells in the bridge.[28] Thus, even the most simple model for the spiro unit cell indicates its enhanced electron mediation properties compared to a linear chain.

For long chains, the amplititude of the wave function in the interior of the molecule changes by the factor ϵ on moving one unit cell in the chain. In spiroalkanes there are two carbon atoms between equivalent points in adjacent unit cells. To first order we can calculate the change in optical or thermal matrix element between donor and acceptor wave functions for any groups connected by the linkers using this fact. For example, when $E = -5.0$, the donor–acceptor overlap changes by a factor of about 0.28 upon adding another CH_2 group to the *n*-alkane. At the same energy the overlap between spiro wave functions changes by a factor of 0.14 upon adding an extra spiro unit. This is an average decay factor of only 0.37 per carbon atom for the spiro linker. The significant difference in decay per carbon atom is a unique feature of the spiro linkage and accounts for the "surprisingly rapid" charge transfer observed by Stein, Lewis, Seitz, and Taube. Table VIII highlights this difference for several energies.

We can use this sort of analysis to compare the attenuation of T_{ab} with distance for a specific linker simply by studying the ϵ vs. E plot. Figure 5a compares the band region in the $\epsilon + 1/\epsilon$ plots for *n*-alkane and spiroalkane. ϵ is the decay per unit cell. Figure 5b shows the ϵ' vs. E plot for the band gap where ϵ' is the decay per carbon atom. Such a divergence from the alkane decay should not occur to such a large degree in the parallel but not frequently intersecting electron-transfer pathways of the steroid derivatives prepared by Calcaterra, Closs, and Miller, for example.[7]

Comparison with Previous Estimates of α. The constant ϵ is related to the decay constant α as shown in Table III. Previous estimations of the energy of the "transferring" electron relative to the medium in which it tunnels have been made. For example, Hopfield estimated $\alpha \simeq 0.72$ Å^{-1} while Jortner suggested $\alpha \simeq 1.3$ Å^{-1} for electron transfer in proteins. It is now clear that this decay depends critically on both the energy of the transferred electron and the detailed structure of the barrier between donor and acceptor. Hopfield's original model assumed a 2-eV barrier height to tunneling. Within our model that means the localized states are 2 eV from either the conduction or valence band (see Figure 5b). In the *n*-alkane model the states 2 eV from the band edges have $\epsilon \sim 0.21$–0.23 or $\alpha = 0.98$ Å^{-1} (through bond) and $\alpha = 1.3$ Å^{-1} (through space; notice comment below Table III).

Redi and Hopfield compared the optical and thermal tunneling matrix elements for two model potentials.[25] They found $T^{op} > T^{th}$, especially at large electron-transfer distances. Their wave functions decay with energy and distance as $\exp(-\sqrt{|E|}R)$. In our calculation $(\epsilon + 1/\epsilon) \simeq 1/\epsilon$ so $|E| \propto 1/\epsilon$ near the band edges. Thus, from eq 12 and Table III the wave function decays with distance and energy as

$$\exp(-|(\ln E)|R)$$

For given E the wave-function decay is always more rapid in the square well or δ well models of Redi and Hopfield. Also, wave-function decay is more sensitive to energy changes in the Redi and Hopfield model. Because of the different dependence of decay on energy, the vibrational relaxation of the localized state produces a greater change in matrix element in the Redi–Hopfield model than in the current model. This serves to decrease the optical matrix with distance more slowly than the thermal matrix element in their model. In the model described here, the optical and thermal tunneling matrix elements are not very different in magnitude (see Tables IV, VI, and VII).

Quantum Chemical Considerations. Our modified tight binding calculation has predicted that electron transfer between ruthenium ions proceeds via hole transfer through the bonding bridge orbitals. Wave function decay is slow for donor and acceptor eigenstates near the band edges. The two actual exchange mechanisms, double exchange (electron transfer via conduction band) and superexchange (hole transfer through the valence band), involve mixing of trap states with linker states.[54,55] Since this mixing involves energy denominators (in first-order perturbation theory) of E(trap) − E(bridge), the strength of the mixing between localized states and linker states is enhanced by their energetic proximity.

An infinite or cyclic chain of spiroalkane orbitals satisfies Bloch's theorem so $\epsilon = \exp(i\vec{k}\cdot\vec{R})$ where $\vec{k}$ is a real reciprocal lattice vector and $\vec{R}$ is a translation vector. In this case $-2 \leq (\epsilon + 1/\epsilon) \leq 2$. We expect (except, perhaps, at points of special symmetry) as many energy roots as basis functions in the unit cell. The six unique orbitals in the spiroalkane give rise to the six bands for $-2 \leq (\epsilon + 1/\epsilon) \leq 2$ in Figure 2. When the linear molecule is truncated, many eigenstates still fall in the range $-2 \leq (\epsilon + 1/\epsilon) \leq 2$ and are well delocalized. Others have ϵ real and correspond to localized states. The singularities in these band-structure plots arise from energy splittings due to orbitals not contributing to C–C bonds.

One could have formulated the boundary conditions of the spiro problem in many other ways. For example, several orbitals on the metals and sulfurs were ignored. Also, a particular geometry was assumed. As long as the position of the sulfur orbitals which participate in the electron transfer do not drastically change in energy, we will be forced to place the localized ruthenium eigenstates very near the valence states and will find similar falloff of T_{ab} with distance. The ability to find this characteristic decay and its dependence on linker geometry is the principal success of this method.

If one believes that the optical absorption reported in the experimental studies promotes an electron between localized states, one must build the ability to adopt local character into the wave functions from the very start. The CNDO/2 method that Stein, Lewis, Seitz, and Baker used to analyze only the linker will not predict the exponential dependence of the charge transfer band extinction coefficient on distance found in these molecules.

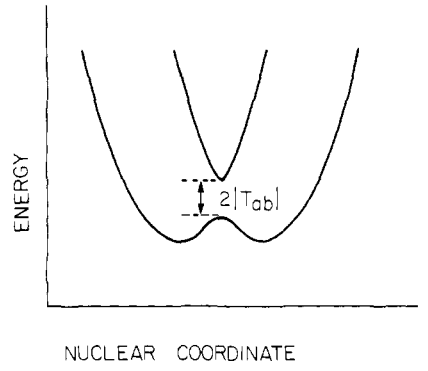

Figure 6. The traditional view of the potential energy surface relevant to electron transfer is shown. The nuclear coordinate represents the metal–ligand and solvent coordinates.

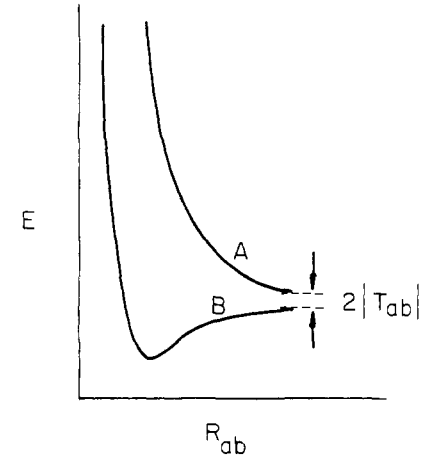

Figure 7. The total energy of the two states, bonding (B) and antibonding (A), formed by a linear combination of two atomic orbitals is shown.

The thermal tunneling matrix element represents the splitting between nuclear potential energy surfaces at the crossing point between reagents and products (Figure 6).[56] The nuclear coordinate in this figure symbolically represents the many metal–ligand and metal–solvent coordinates. The size of $\mathbf{T}_{ab}$ varies with the metal–metal distance in a fashion shown in Figure 7. We notice from Table VII that the thermal tunneling matrix element decreases with distance but never changes sign. In a two-orbital, one-electron model of electron transfer this energy splitting must not change sign with distance. A sign change implies a crossing of the bonding and antibonding energy surfaces (Figure 7). Such a crossing is forbidden by the nodal theorem.[57] That is, since the ground state is nodeless and since higher states have nodes, $E_g < E_{ex}$ for any internuclear separation. When intervening orbitals between donor and acceptor are introduced, the sign of T_{ab} may vary with transfer distance. For example, in Figure 4c we see that ϵ for *n*-alkane is negative so the sign of $\mathbf{T}_{ab}$ alternates as the number of bridging carbon atoms is increased. However, within our model $|\mathbf{T}_{ab}|^2$ is still a monotonically decreasing function of donor acceptor separation, which may only be changed in integral steps. Newton has calculated the tunneling matrix element for electron exchange between hexaquo Fe(II) and Fe(III) using ab initio quantum mechanical methods.[58] He finds a node in $\mathbf{T}_{ab}$ for an internuclear iron distance of 7.6 Å. Thus, either there is an unusual many-body effect at work or his method incorrectly

(54) Halpern, J.; Orgel, L. *Discuss. Faraday Soc.* **1960**, *29*, 32–41.
(55) Ratner, M. A.; Ondrechen, M. J. *Mol. Phys.* **1976**, *32*, 1233–1245.
(56) Marcus, R. A. *Annu. Rev. Phys. Chem.* **1964**, *15*, 155–196.
(57) Messiah, A. "Quantum Mechanics"; Wiley: New York, 1958; Vol. 1 pp 109–110.
(58) Newton, M. D. *Int. J. Quantum Chem.: Quantum Chem. Symp.* **1980**, *14*, 363–391.

calculates the long-range wave function decay.

Our method does have severe limitations. It is a one-electron approximation and has the flaws of the standard Hückel techniques.[39,52,59] Transition and dipole moments calculated from Hückel wave functions are not always reliable. However, to the extent that the "odd" electron in the electron-transfer calculation is in a very different eigenstate compared with the other electrons in the molecule, this approximation may be better than expected. The omnipresent problem of selecting appropriate, consistent parameters is obvious in this calculation. Particularly annoying is the difficulty of treating transition metals within the one-electron approximation.

Biological Applications of This Theory. The techniques described in this paper are applicable to electron-transfer processes where the through-bond rather than through-space electron-transfer pathway dominates. The method requires knowledge of the energy of the "transferred" electron relative to the bridge states. The question of through-bond vs. through-space pathways in metal-labeled proteins is an important one.[60,61] Our method allows prediction of the changes in electron-transfer rate as a function of redox energy and through-bond distance. To study through-bond effects on long-distance electron transfer in proteins, one would like to roughly fix the through-space distance between donor and acceptor and vary only the number of through-bond links between the centers. Perhaps binding of metals to the surface of a roughly spherical protein with a redox group in its center would be appropriate. Such an experiment would show the importance of through-bond interactions (and the usefulness of this theory) in electron transfer through proteins.

For the mixed-valence spiro molecules the experimental value of ϵ for Ru^{2+} is $\sim$0.4–0.47 or $\epsilon' \simeq 0.65$ (recall $\epsilon' = \epsilon^{1/2}$). This value of ϵ corresponds to $E = -6.5$ eV. The redox potentials of these molecules are $\sim$+0.5V vs. NHE; however, the redox energy corresponds to thermal charge transfer so we also have $\sim$0.75 eV of relaxation energy to include. Using these facts we may correlate the redox potential and decay constant for spiro and other saturated linkers. By changing the sign of the energy scale in Figure 5b, placing the redox energy of +0.5V vs. NHE at −5.75 eV (−6.5 + 0.75) eV on that figure, and converting from ϵ to α we find Figures 8a and 8b. These describe the decay constant as a function of redox energy for the *n*-alkane. Now if we consider the alkane backbone to be a fair model for the protein backbone, we may calculate α for a given number of peptide unit cells.

Electron transfer between native and modified proteins occurs in an activated complex with electronic energy $E^{el} \simeq (E_d + E_a)/2$ where E^{el} is the energy appropriate for use in Figure 8. E_d and E_a are the redox energies of the separated ligated metals.

Assuming two redox centers are known to be separated by X Å, a "taut" alkane chain between the center and the chain would contain $N = (2X)/(2.4)$ carbon atoms. The tunneling matrix element for this linkage would be

$$\exp[-\alpha(E^{el})N(1.54)] \qquad (13)$$

$\alpha(E^{el})$ is the through-bond decay constant appropriate to the activated complex (read from Figure 8a). *This should be the upper limit of the bond-mediated tunneling matrix element.* Calculation of matrix elements through longer chains requires only knowledge of N and E^{el}. For example, in the pentaammine ruthenium(III) (histidine-33)–ferricytochrome prepared by Gray and co-workers, $E^{el} = 0.21$ V vs. NHE, $X = 15$ Å, $N = 12.5$ so $T_{ab}^{max} \simeq \exp[-(0.69)(12.5)(1.54)] \simeq 1.7 \times 10^{-6}$ eV. Since the transfer probably does not occur through such a taut structure and T_{ab} decreases by a factor of $\exp[-(0.69)(1.54)(3)] \simeq 0.04$ per amino acid residue, it is unlikely that the dominant pathway in this protein with this choice of metals is a purely bond-mediated one. However, if the more favorable energetic regions (near the band edges) are accessible, a through-bond pathway may become more important.

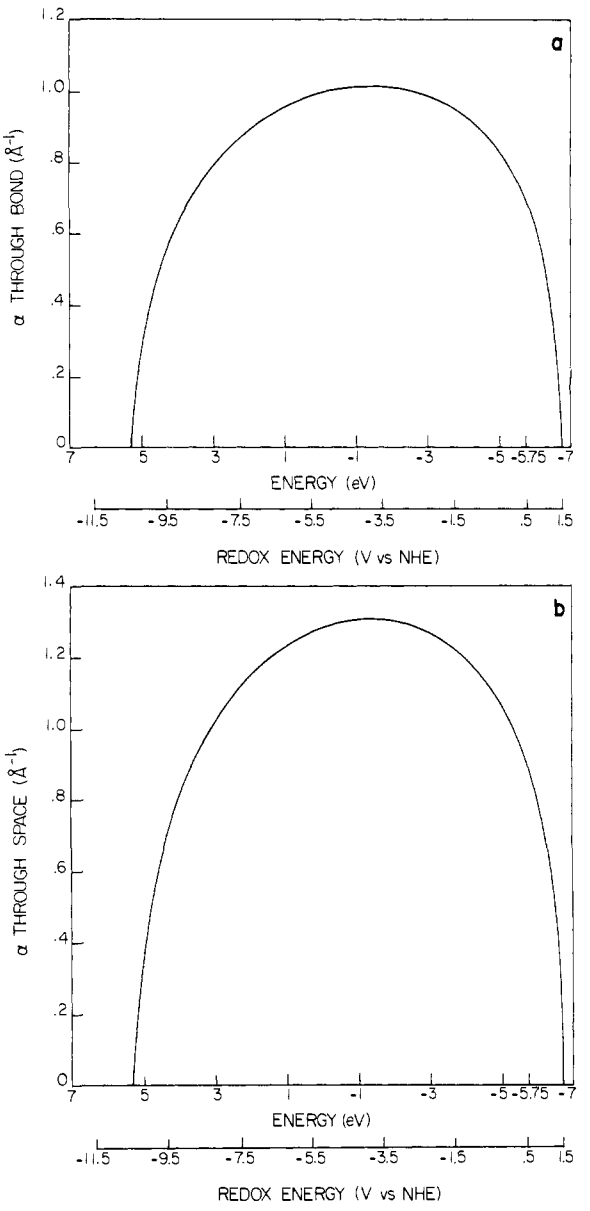

Figure 8. The dependence of thermal matrix element decay constant (α) as a function of the redox energy of the activated complex is shown: (a) when distance is measured through bond for an alkane chain, (b) when distance is measured through space for a "taut" alkane chain.

Calculations exploiting the periodic nature of other saturated rigid linkers are now being carried out. Similar calculations on polypeptide backbone are also underway. With this method we hope to achieve a better understanding of the role of bridge geometry and donor/acceptor energetics on the electronic tunneling matrix element.

T_{ab} and "Inverted Behavior". In this paper we have considered only the *electronic* contribution to the electron-transfer rate. The actual rate is, within the Franck–Condon and Born–Oppenheimer approximations, a product of nuclear and electronic factors. In I–IV the nuclear factors should be approximately equal so a comparison of $|T_{ab}|^2$ may be used to predict ratios of transfer rates.

Both the optical and thermal tunneling matrix elements are quite sensitive to the energies of the donor and acceptor localized states with respect to the bridge states. Therefore, when comparing transfer rate as a function of reaction driving force, one must realize that changing reaction energetics may in fact change the size of T_{ab} (depending on the position of the localized states in the band gap). For this reason, when looking for the "inverted region" in families of molecules, one must also consider the change

(59) Sinanoğlu, O.; Wiberg, K. B. "Sigma Molecular Orbital Theory"; Yale University Press: New Haven, 1970.
(60) Margalit, R.; Pecht, I.; Gray, H. B. *J. Am. Chem. Soc.* **1983**, *105*, 301–302.
(61) Winkler, J. R.; Nocera, D. G.; Yocom, K. M.; Bordignon, E.; Gray, H. B. *J. Am. Chem. Soc.* **1982**, *104*, 5798–5800.

in the *electronic* contribution to the rate with driving force.[62,63] Depending on the energy of the localized states, a misinterpretation of the data may result if T_{ab} is assumed constant. Future work will attempt to include a model for nuclear motion.

Conclusions

We have shown that semiempirical quantum chemical techniques predict the dependence of tunneling matrix element on distance and linker geometry. The localized states used in these calculations must have the proper exponential decay in order to calculate meaningful rates. To the extent that the linkers create periodic potentials for the electrons, we are assured of obtaining proper wave-function decay in these calculations. There are two major qualities of the method that make it especially appealing. It allows direct study of the effect of linker geometry on the electronic tunneling matrix element. The method also allows systematic study of the effect of donor and acceptor redox level on the electronic tunnelling matrix element. It is hoped that the synthesis of other rigidly linked, weakly interacting electron donor-acceptor molecules will provide further tests of this theory.

Acknowledgment. The authors are grateful to Dr. N. Agmon, Dr. R. A. Marcus, Mr. J. N. Onuchic, and Dr. M. A. Ratner for very helpful suggestions with regard to this manuscript. This research was supported in part by NSF Grant No. DMR-8107494.

Registry No. I, 76723-23-4; II, 81205-53-0; III, 81205-54-1; IV, 88548-86-1.

(62) Marcus, R. A.; Siders, P. *J. Phys. Chem.* **1982**, *86*, 622-630.
(63) Beitz, J. V.; Miller, J. R. *J. Chem. Phys.* **1979**, *71*, 4579-4595.

Bonded and Nonbonded Charge Concentrations and Their Relation to Molecular Geometry and Reactivity

R. F. W. Bader,* P. J. MacDougall, and C. D. H. Lau

Contribution from the Department of Chemistry, McMaster University, Hamilton, Ontario, Canada L8S 4M1. *Received August 12, 1983*

Abstract: The Laplacian of the charge density, the quantity $\nabla^2\rho(\mathbf{r})$, determines the regions of space wherein electronic charge is locally concentrated and depleted. This function demonstrates, without recourse to any orbital model or arbitrary reference state, the existence of local concentrations of electronic charge in both the bonded and nonbonded regions of an atom in a molecule. The form of the Laplacian of ρ for an isolated atom reflects its shell structure by exhibiting a corresponding number of pairs of spherical shells of alternating charge concentration and charge depletion. The uniform valence shell of charge concentration is distorted upon chemical combination through the creation of local maxima within this shell. The numbers, locations, and relative sizes of the bonded and nonbonded concentrations of charge in the valence shell of a bonded atom as determined by the Laplacian of ρ are found to be in general agreement with the corresponding properties that are ascribed to bonded and nonbonded electron pairs in models of electronic structure and, particularly, in Gillespie's VSEPR model of molecular geometry. Examples are considered which contain three (SO_2), four (CH_4, SiH_4, NH_3, PH_3, OH_2, SH_2, NF_3, PF_3, $ClCl_2^+$, ClF_2^+), five (ClF_3, SF_4, SF_4O), and six (ClF_5) local concentrations of electronic charge in the valence shell of the central atom. It is also shown that the regions of maximum electronic charge concentration and depletion as determined by the Laplacian of ρ correlate respectively with the positions of electrophilic and nucleophilic attack. Nucleophilic attack at a carbonyl carbon, for example, is predicted to occur from above or below the plane of the nuclei along lines of approach forming an angle of $\sim 110°$ with the C=O bond axis. The Laplacian of ρ gives physical expression to the electron-pair concept of Lewis. This same function relates the local form of the charge density to the mechanics which govern it. Thus one may attempt through its use to obtain a deeper understanding of the models of molecular geometry and reactivity that make use of the electron-pair concept.

I. Introduction

The gradient vector field of the charge density, the field $\nabla\rho(\mathbf{r})$, determines the structure and structural stability of a molecular system.[1] In terms of the *global* behavior of this field, one may define the atoms[2] and the set of atomic interactions present in a molecule.[3,4] The Laplacian distribution of the charge density, the field $\nabla^2\rho(\mathbf{r})$, identifies the regions of space wherein the electronic charge of a molecule is locally concentrated and depleted.[5] The Laplacian of $\rho(\mathbf{r})$, as well as providing this enhanced view of the *local* form of the charge density, relates this form to the quantum mechanical equations which govern the behavior of $\rho(\mathbf{r})$.[6,7] In particular, the sign of the Laplacian of $\rho(\mathbf{r})$ determines the relative magnitudes of the local contributions of the potential and kinetic energy densities to their virial theorem averages. By obtaining a map of those regions where $\nabla^2\rho(\mathbf{r}) < 0$, the regions where electronic charge is concentrated, one obtains a map of the regions where the potential energy makes its dominant contributions to the energy of a system.[5]

The Laplacian distribution of a molecular charge distribution demonstrates the existence of local concentrations of electronic charge in both the bonded and nonbonded regions of an atom in a molecule. This information is obtained without recourse to any orbital model or arbitrary reference state. The ability to locate

(1) Bader, R. F. W.; Nguyen-Dang, T. T.; Tal, Y. *Rep. Prog. Phys.* **1981**, *44*, 893-948.
(2) Bader, R. F. W.; Beddall, P. M. *J. Chem. Phys.* **1972**, *56*, 3320-3329.
(3) Bader, R. F. W.; Anderson, S. G.; Duke, A. J. *J. Am. Chem. Soc.* **1979**, *101*, 1389-1395.
(4) Bader, R. F. W.; Nguyen-Dang, T. T.; Tal, Y. *J. Chem. Phys.* **1979**, *70*, 4316-4329.
(5) Bader, R. F. W.; Essén, H. *J. Chem. Phys.*, in press.
(6) Bader, R. F. W.; Nguyen-Dang, T. T. *Adv. Quantum Chem.* **1981**, *14*, 63-124.
(7) Bader, R. F. W.; Essén, H. "Local Density Approximations in Quantum and Solid State Physics"; Dahl, J. P., Avery, J., Ed.; Plenum Press: New York, 1983.

0002-7863/84/1506-1594$01.50/0